Rock Mechanics, Nelson & Laubach (eds) © 1994 Balkema, Rotterdam, ISBN 90 5410 380 8

Tensile properties of rocks in four-point beam tests under confining pressure

Ram Weinberger, Ze'ev Reches & Amir Eidelman
School of Geology and Geophysics, University of Oklahoma, Norman, Okla., USA (Presently: Department of Geology, Hebrew University, Jerusalem, Israel)
Thurman E. Scott
School of Geology and Geophysics, University of Oklahoma, Norman, Okla., USA

ABSTRACT: The strength and elastic properties of rocks were measured with a four-point beam device placed inside a pressure vessel. The experiments were conducted with Tennessee sandstone, Indiana limestone, and Berea sandstone. The tensile Young's modulus is nonlinear and best represented by $\sigma_t = A\ \varepsilon_t^B$, where σ_t, ε_t are the tensile stress and tensile strain and A and B are constants. B ranges from 0.56 for tests without confinement to 0.85-0.9 for tests with confinement of 10 MPa or more. The tensile strength depends only slightly on the confining pressure and it ranges from -8.8 MPa to -5.1 MPa. The yielding envelope agrees with the parabolic shape predicted by Griffith. The fractures observed under 20 MPa of confinment are invariably tensile with no indication for transition to shear fractures (faults).

INTRODUCTION

The mechanical properties of rocks strongly depend on the sign of applied loads: tensile versus compressive. For example, the tensile strength of rocks and rock-like materials is 8-10 times smaller then their compressive strength (Griffith, 1921). Therefore, the tensile strength and tensile elastic moduli, should be determined under tensile stress conditions. Probably the most comprehensive series of experiments in the tensile regime was published by Brace (1964). He used a "dog bone" design for his samples and loaded them in a standard triaxial cell under extension conditions in which the confining pressure was larger then the axial stress. Brace could also generate axial tension on his samples. Similar loading conditions were used in the experiments of Griggs and Handin (1960).

It is experimentally difficult to determine the tensile properties of rocks under confining pressure, and tensile strength and tensile moduli are usually determined under room pressure (e.g., plate splitting, Brazilian test, four-point beam). We measured the tensile strength and tensile elastic properties of three rocks under confining pressure by using a four-point device placed inside a pressure vessel (Fig. 1). Four-points beam tests are a simple and effective method to measure the tensile properties of metals and rocks (e. g., Nadai, 1950; Oldroyd, 1971). Experiments with the four-point device generated excellent agreement with the results of uniaxial tests for metals (Yokoyama, 1988). In the present tests the beam samples were deformed under confining pressure and provided the tensile properties of the rocks for polyaxial stress states.

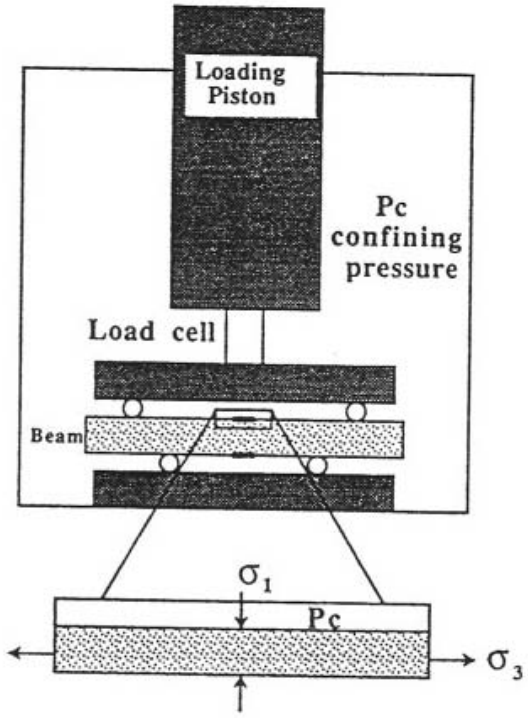

Figure 1. Schematic presentation of the experimental setting that includes a four-point device and a beam inside a pressure vessel. Note the strain gauges on top and bottom of the beam. σ_1 and σ_3 are the maximum and minimum compressive stresses.

EXPERIMENTAL APPROACH

The four-point bend test is a relatively simple method to simultaneously determine the compressive and tensile elastic moduli. Yokoyama (1988) derived a useful formulation for the stress-strain relations in a four-point bending test. His analysis utilizes the experimental measurements of the axial load, P, the strains at the top and bottom of the beam, and the geometry of the device and the beam. The derivations of Yokoyama (1988) lead to the following values of σ_t and σ_c, the maximum tensile stress and the maximum compressive stress along the beam (fiber stresses),

$$\sigma_t = \frac{dM(\epsilon_t + \epsilon_c) + 2M(d\epsilon_t + d\epsilon_c)}{bh^2 d\epsilon_t} \qquad \sigma_c = \frac{dM(\epsilon_t + \epsilon_c) + 2M(d\epsilon_t + d\epsilon_c)}{bh^2 d\epsilon_c}$$

where $M = 0.5\,P\,(L_t - L_c)$ is the bending moment of the beam (L_t and L_c are the spacing of the pairs of the loading points for the tensile side and for the compressive side, respectively); ε_t and ε_c are the tensile and compressive strains measured at the top and bottom of the deformed beam, respectively (fiber strains); b is the beam width; h is the beam height; dM, $d\varepsilon_t$ and $d\varepsilon_c$ are the increments of the moment and the strains during the experiment (the differentials between two consecutive steps in the experiment). We used the last set of equations to calculate the stress-strain curves for both tension and compression from the experimental data of P, ε_t and ε_c.

Sample Preparation. Twenty experiments were conducted with three rock types: Tennessee sandstone of 6% porosity (eight tests), Indiana limestone (eight tests), and Berea sandstone of 17-19% porosity (four tests). Samples were machined into 15.0 cm long rectangular beams with cross sectional dimensions of 1.8 cm by 1.8 cm. The surfaces were grounded parallel to within 0.001 cm under dry conditions with an 80 grit aluminum oxide wheel. Two strain gauges were mounted parallel to the long axis of the beam surfaces for monitoring the axial strain (Fig. 1). The beams tested under confining pressure were jacketed with heat shrink polyolefin tubing.

Experimental Setting. We used a four-point beam device that was designed and built in the Halliburton Laboratory, University of Oklahoma, Norman, by Bjornen (1994) following Yokoyama (1988). Unconfined tests were run on a MTS 319 load frame. Tests under confining pressure were performed on the servo-controlled MTS Model 315 load frame with an integral MTS 138 MPa (20,000 psi) pressure vessel. The axial load P, was measured with a sensitive internal load cell and the beam parallel strains were measured with the stain gauges at top and bottom (Fig. 1). The benchmarking with aluminum (6061) beam yielded accuracy smaller than 1% in the strain measurements.

Data acquisition was controlled by an IBM-PC 486. We used a Hewlett-Packard 3497a for data acquisition/control unit. It acquired parameters for storage at 1 second intervals during the test. The parameters were recorded as voltage values of the axial load, axial stroke, confining pressure, tensional strain(s) and compressional strain(s).

The experimental conditions are listed in Table 1. All samples were room dry and were deformed at room temperature. The confining pressure ranges from 5-20 MPa, with one experiment under 50 MPa. A typical experiment lasted 30-50 minutes under constant stroke rate. The strain rates monitored from the strain gauges were approximately 10^{-6} sec^{-1}.

RESULTS

Elastic Moduli

The tensile and compressive stresses within the beams were calculated from the measured axial load, P, and the strains measured at the top and bottom of the beam, ε_t and ε_c. Representative stress-strain curves are shown in Fig. 2 for the three tested rocks. Almost all curves are relatively smooth in their initial part, up to a tensile strain of 0.0001-0.0003. At larger strain values, both σ_t and σ_c curves become crooked and the intensity of the irregularities increases with the strain increase (Fig. 2). The smooth, initial curves indicate elastic deformation whereas the subsequent stress irregularities indicate local microcracking. In all experiments the compressive stress-strain curves are generally linear and the tensile stress-strain curves are generally nonlinear (Fig. 2). Accordingly, we fit linear coefficients to the compressive curves, and the relations of $\sigma_t = A\ \varepsilon_t^B$ to the tensile curves (Table 1). All curve fittings were with correlation coefficients of $r > 0.98$.

The compressive Young's modulus for Tennessee sandstone is 19,000 to 40,000 MPa, with some consistent increase with confinement (Table 1), in good agreement with those of Scott and Nielsen (1991). The compressive Young's modulus for Indiana limestone is 30,600 ± 3,900 MPa with no dependence on the confining pressure. The

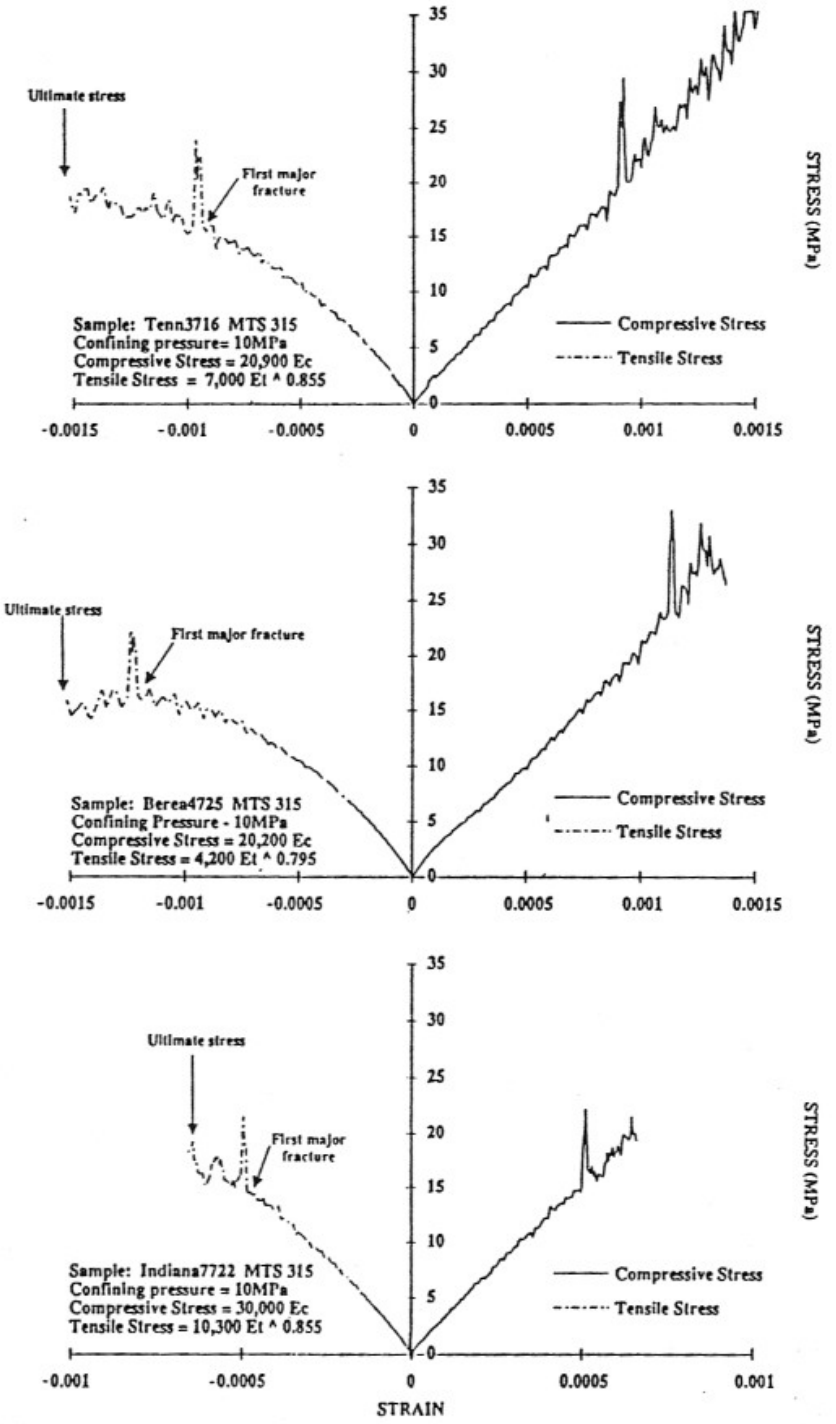

Figure 2. Stress-strain curves of three tests under confining pressure of P_c= 10 MPa. The tensile and compressive stresses σ_t and σ_c are plotted versus the corresponding strains ε_t and ε_c , tensile curve on the left (negative strain) and compressive curve on the right (positive strain). Note that while tensile stresses are negative, both tensile and compressive stresses are plotted as absolute values. The principal stresses at the surface of the convex side of the beam are: $\sigma_1 = P_c$ and $\sigma_3 = -(\sigma_t - P_c)$; the principal stresses at the surface of the concave side of the beam are: $\sigma_1 = (\sigma_c + P_c)$ and $\sigma_3 = P_c$. The experimental data and the coefficients of the elastic moduli appear in the lower left part of each figure.

Table 1. Experimental conditions and results.

Test #	Confining pressure (MPa)	Compressive modulus (MPa)	A-Tensile slope (MPa)	B-Power of tensile curve	Tensile strain at yielding	Tensile Strength (MPa) Lower (3)	Upper (4)
INDIANA LIMESTONE							
24A	0.1	26,600	4,000	0.82	0.00041	-5.3	-5.3
24B	0.1	29,100	3,600	0.80	0.00041	-6.2	-6.2
3720	5	34,900	8,000	0.86	0.00054	-5.9	-5.9
8722	5	28,600	23,500	0.99	0.00038	-3.6	-7.4
7722	10	30,000	10,300	0.86	0.00048	-4.6	-8.2
5722	20	37,200	22,000	0.94	0.00053	2.6	-5.9
9803	20	28,200	16,000	0.91	0.00100	-4.6	-4.6
4716	10	N/A	N/A				
Mean (1)		30,657			0.00054	-3.9	-6.2
STD (1)		3,882			0.00021	3.0	1.2
BEREA SANDSTONE							
24A	0.1	10,200	170	0.56	0.00109	-3.2	-3.8
6810	5	26,100	6,400	0.83	0.00069	-8.6	-9.8
4725	10	20,200	4,200	0.80	0.00121	-6.3	-6.9
5803	10	27,500	4,800	0.80	0.00105	-7.4	-9.5
Mean		21,000			0.00101	-6.4	-7.5
STD		7,864			0.00022	2.3	2.8
TENNESSEE SANDSTONE							
24A	0.1	22,600	350	0.56	0.00113	-7.1	-7.1
24B	0.1	16,300	1,100	0.66	0.00081	-9.4	-9.4
5722	5	25,000	5,000	0.85	0.00066	-8.4	-15.6
8803	5	22,800	3,200	0.75	0.00095	-10.0	-14.1
3716	10	20,900	7,000	0.86	0.00093	-5.8	-9.1
9803	10	24,000	4,900	0.79	0.00072	-4.3	-9.1
6722	20	31,500	12,500	0.87	0.00093	-5.4	-8.1
7727	50	40,400	14,600	0.86	0.00099	14.1	-18.2
Mean (2)		25,438			0.00088	-7.2	-10.4
STD (2)		7,387			0.00016	2.2	3.2

(1) Not including experiment 4716 (2) Not including experiment 7727
(3) First major fracture (4) Ultimate stress

modulus for the Berea sandstone range from 10,000 MPa to 27,000 MPa with slight dependence on the confining pressure (Table 1). The tensile modulus is represented by the constants A and B. The Berea and Tennessee sandstones have similar A and B. A ranges from ≈ 1,000 MPa at room pressure to ≈ 14,000 MPa at 50 MPa; B ranges from 0.56 for room pressure to 0.85-0.9 for tests with confinement of 10 MPa or more. A and B of Indiana limestone has no clear relation to the confinement (Table 1).

Tensile Strength

The deformed beams were first examined with a binocular, thin sections were prepared from selected regions, and these sections were analyzed with a petrographic microscope (Fig. 3). We traced the fractures on two surfaces to obtain their 3-D shape: the top surface which is the surface with the maximum tensile stress (A, B in Fig. 3), and the sides of the sample (C in Fig. 3).

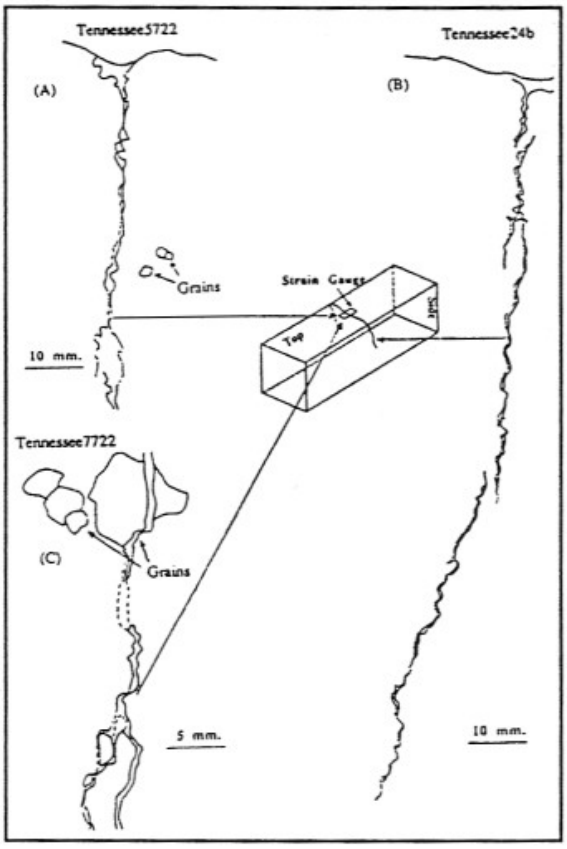

Figure 3 (above). Micrographic view of some tensile fractures in three tests of Tennessee sandstone marked on the figure. Note the crooked shape of the fractures as they bypass the quartz grains.

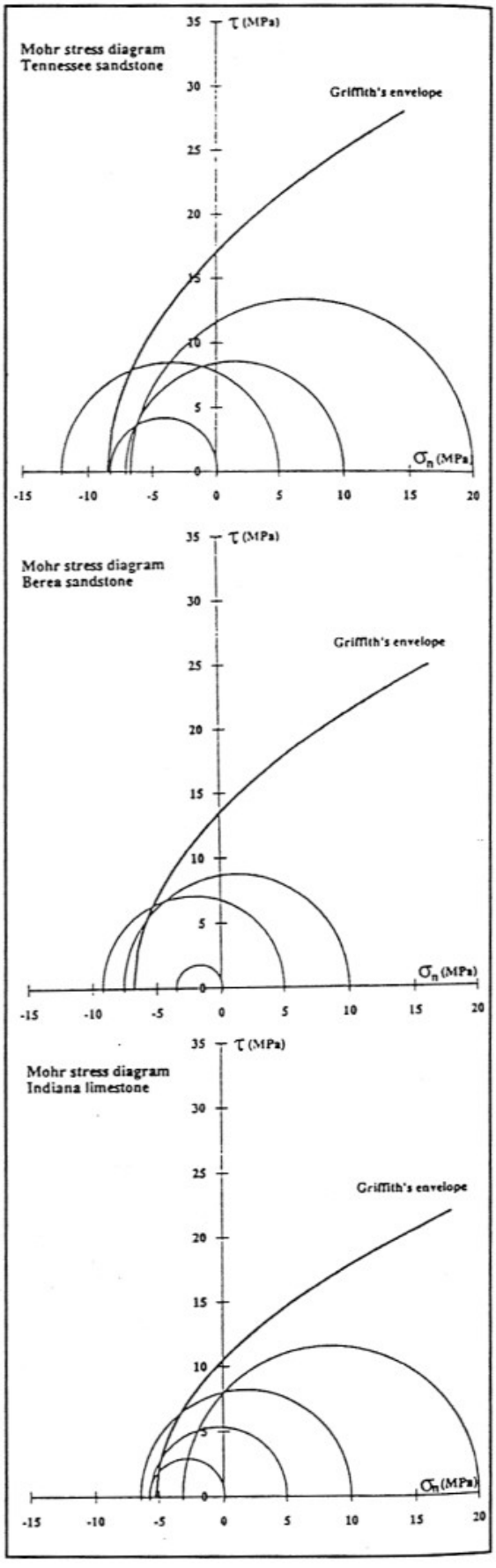

Figure 4 (right). The σ_1 and σ_3 magnitude during the tensile yielding in the present tests plotted on Mohr diagrams. The tensile strength is the mean value of the lower and upper bound for the given confining pressure (see text). Solid, heavy lines are the apparent yielding envelopes calculated according to Griffith. Rock type marked on figures.

Almost all strain-stress curves display irregular curves of σ_t and σ_c for tensile strain larger then 0.0001 to 0.0003; the irregularities increase with increasing strain (Fig. 2). We interpret these irregularities as local, stable fracturing. These fractures initiate at the tensile surface of the beam, where the tensile stresses are the highest, and they propagate into the inner part of the beam. These early fractures grow stably, and they were arrested as they approach the neutral surface of the beam (Fig. 3). Eventually, the sample fails at the ultimate stress (Fig. 2).

Therefore, it appears that the rock beams display two modes of tensile yielding: local, stable fracturing during the early stage, and unstable, crosscutting fracturing during the final stage. We regard the tensile stress of the first major local fracturing (marked in Fig. 2) as the lower bound of the tensile strength and the ultimate stress as the upper bound. The first major fracture is associated with a major stress change as shown in Fig. 2. Thus, for each test we derived a lower and upper bound on the tensile strength (Table 1) and we used the mean value of these bounds as the tensile strength. We found that the tensile strength, S_t, is -8.8 ± 3.1 MPa for Tennessee sandstone, -5.1 ± 2.5 MPa for Indiana limestone and -6.9 ± 2.4 MPa for Berea sandstone (tensile stress is negative) (Table 1).

These results are plotted on Mohr diagrams (Fig. 4). We traced the parabolic yielding envelope of Griffith, $\tau^2 = 4\ S_t\ (\sigma_n + S_t)$ (heavy curves in Fig. 4). This curve fits the stress circles and the observation that the fractures are tensile (normal to maximum tension in Fig. 3). It should be noted that the tensile part of the yielding envelope is usually extrapolated, and only seldom is it bounded by experimental data, for example by Brace (1964). This figure also shows that the tensile strength does not depend on σ_1, the confining pressure. This observation is in good agreement with the experimental results of Brace (1964, Table 4) for several other rock types.

Another interesting problem is the enigmatic transition from tensile fractures (joints) to shear fractures (faults). The present observations indicate that within the range of tested confining pressures (up to 20 MPa), all fractures are tensile fractures with no indication to "hybrid" or transitional fractures. This result is in agreements with the conclusions of Griggs and Handin (1960) and Brace (1964).

CONCLUSIONS

A. It is feasible to run four-point bending tests under confining pressure. This design can provided the tensile strength of the tested rocks and their tensile elastic moduli for confining conditions.

B. The tensile elastic modulus is invariably nonlinear and could be fitted by the form $\sigma_t = A\ \varepsilon_t^B$. Microcracking initiates after strain of approximately 0.0003. In the present beam configuration, this early microcracking is stable and does not cause global yielding, and it drives the stress-strain curves into irregular shape.

C. The tensile strength of the three tested rocks apparently does not depend on the confining pressure.

D. The yielding envelope in the tensile regime of the Mohr diagram seems to agree, in general, with the parabolic shape predicted by Griffith's theory and it does not agree with the predictions of Coulomb criterion.

E. The fractures observed under 20 MPa of confining pressure are invariably tensile in character with no indication for transition to shear fractures (faults).

ACKNOWLEDGEMENTS

The advise, help and suggestions of several people made this work possible. In particular, Lou Boldt who suggested to use bending device inside a pressure vessel and Kevin Bjornen who kindly provided the four-point device built by him. We also wish to thank Carla Cates, David Snyder, Karen Hogan, Peter Lemmon and Tony Haas for their technical support and advise.

The study was conducted as part of the Rock Mechanics Consortium, University of Oklahoma, Norman. It was originally submitted as Report 22A of the Consortium.

BIBLIOGRAPHY

Bjornen, K., 1994. Epoxyl-lastic material used in large scale fluid loss test. M.Sc. Thesis, Univ. of Oklahoma (in preparation).

Brace, W. F., 1964, Brittle fracture of rocks, in William, R. J., ed., *State of stress in the earth's crust*: New York, US, Elsevier, p. 111-174.

Griffith, A. A., 1921. The phenomena of rupture and flow in solids, *Philos. Trans. R. Soc. London Ser. A*, 221, 163-198.

Griggs D. and Handin, J., 1960. Observation of fracture and a hypothesis of earthquakes, *GSA Mem.*, 79, 347-362.

Nadai, A., 1950. *Theory of flow and fracture of solids*, McGraw-Hill, New York, pp. 353-359.

Oldroyd, P. W. J., 1971, Tension-Compression stress-strain curves from bending tests, *J. of Strain Analysis*, 6, 286-292.

Scott, T. E. and Nielsen K.C., 1991, The effects of porosity on the brittle-ductile transition in sandstones, *J. Geophy. Res.*, 96, 405-414.

Yokoyama, T.A., 1988. A microcomputer-aided four-point test system for determining uniaxial stress-strain curves, *J. of Testing and Evaluation*, 16, 198-204.